Supporting Information

Stanford et al. 10.1073/pnas.1205028109

SI Materials and Methods

Reagents. Sodium orthovanadate was purchased from Sigma. Alexa Fluor 555-dextran, Sytox Orange, CellMask Deep Red, and LIVE/DEAD Fixable Red or Near-IR Dead Cell Stain Kits were purchased from Invitrogen. Recombinant protein phosphatase 1 (PP1) was purchased from Upstate/Millipore. Recombinant protein phosphatase 2A (PP2A) and 2B (PP2B) were purchased from Calbiochem/EMD. Recombinant CD45, T-cell tyrosine phosphatase (TC-PTP), SHP-1, and protein tyrosine phosphatase 1B (PTP1B) were purchased from Enzo Life Sciences International. The allophycocyanin-conjugated anti-CD45 antibody was purchased from Biolegend. Alexa Fluor 488-conjugated anti–phospho-Lck (Y505) and anti–phospho-Src (Y418) antibodies and all other reagents for phospho-flow cytometry were purchased from BD Biosciences. The anti-CD45 antibody used in Western blotting was purchased from Epitomics. The anti-LYP and anti–TC-PTP antibodies used in Western blotting were purchased from R&D Systems. The anti-CD3, clone OKT3, was purchased from eBioscience. The FITC-conjugated anti-CD69 antibody was purchased from Biolegend. The anti-GAPDH antibody used in Western blotting was purchased from Cell Signaling Technology. The nonnatural amino acid phosphorylated coumaryl amino propionic acid (pCAP) was synthesized as previously reported (1). The CD45 inhibitor NSC 95397 (2, 3), the TC-PTP inhibitor compound 8 (4), and the LYP inhibitor compound 4 (5) have been described previously. Analogs of NSC 95397 were obtained from the National Cancer Institute Open Chemical Repository or were purchased from Sigma. The Spectrum Collection compounds were purchased from MicroSource Delivery Systems.

Fluorenylmethoxycarbonyl (Fmoc)-protected amino acids, Rink amide AM resin, and 2-(6-chloro-1H-benzotriazole-1-yl)-1,1,3,3-tetramethylaminium hexafluorophosphate (HCTU) were purchased from Novabiochem. N,*N*-Dimethylformamide (DMF), trifluoroacetic acid (TFA), and 1,8-Diazabicyclo[5.4.0]undec7-ene (DBU) were purchased from Alfa Aesar. Diisopropylcarbodiimide (DICI) and triisopropylsilane (TIS) were purchased from Acros Organics. Diisopropylethylamine (DIPEA), trimethylsilyliodide (TMSI), dichloromethane (DCM), methanol, and acetic acid were purchased from Fisher Scientific. 1-Hydroxybenzotriazole (HOBT) was purchased from Chem-Impex. All reagents were used without further purification.

Peptide Synthesis. A summary of peptide sequences is shown in Table S2. Peptide-synthesis vessels were comprised of a fritted column purchased from Whatman Inc., Teflon stopcock and cap purchased from Applied Separations. Peptides were purified on a Varian ProStar 210 preparative-scale HPLC and characterized by MALDI-TOF on a DE-STR (PerSeptive Biosystems/ABI) instrument by the University of Utah Mass Spectrometry and Proteomics Core Facility using α-cyano-4-hydroxycinnamic acid as a matrix.

Synthesis of peptide 1, peptide 1b, and peptide 1c, general sequence Ac-EDNE-X-TARE-NH_2 where X = pCAP, CAP, and Et_2-pCAP and CAP-R_8. Rink amide AM resin (50 mg, 0.035 mmol) was preswelled in 1 mL DMF in the peptide-synthesis vessel and shaken for 30 min. After draining, 1 mL of 2% DBU in DMF was added and was shaken for 30 min. The solution was drained, and another 1 mL of 2% DBU was added and shaken for an additional 30 min. The fully deprotected resin then was washed three times with 1 mL DMF. The desired amino acid [three equivalents (equiv)] was dissolved in 1 mL DMF along with HOBT and DICI (0.105 mmol, three equiv each) and allowed to sit for 10 min. The mixture was added to the rinsed resin and shaken vigorously for 3 h. After coupling, the solution was drained and rinsed three times with 1 mL DMF and deprotected with 1 mL 2% DBU (2× 30 min). Then the next amino acid was coupled, and the cycle was repeated until each amino acid had been added. The amino acid N-terminal to X was coupled twice to ensure a complete reaction. The first coupling was performed using the conditions described above, rinsed three times with 1 mL DMF, coupled a second time using five equiv of amino acid, HCTU (0.175 mmol, five equiv), and DIPEA (0.35 mmol, 10 equiv), and shaken for 1.5 h. After deprotection of the final amino acid with 2% DBU, the N terminus was acetylated using acetic acid/HCTU/DIPEA (five equiv, five equiv, and 10 equiv, respectively) for 1.5 h. The resin then was washed three times with 1 mL DMF and three times with 1 mL DCM and dried under vacuum. The pCAP-containing peptides (but not the CAP or Et_2pCAP peptides) were deprotected with a 1-M solution of TMSI in DCM for 1 h. The resin then was washed three times with 1 mL DCM and three times with 1 mL methanol and dried under vacuum. The peptides then were cleaved from the resin using a cleavage mixture containing 95% TFA, 2.5% water, and 2.5% TIS for 4 h. The peptides were collected under vacuum. The resin was rinsed with 1 mL TFA and 10 mL water. The collected solution was diluted with ∼40 mL water and lyophilized. The peptides then were purified on HPLC using water, acetonitrile, and TFA buffers and were lyophilized again. The peptides were characterized using MALDI-TOF MS.

Synthesis of C_n-βAla-R_7-CAP-NH_2 (C_n-R_7-CAP) peptides, where n = 14, 16, 18, or 20. C_{14}-R_7-CAP (CAP-CPP) was purchased from 21st Century Biochemicals or was synthesized according to the procedures described below. C_{16}-R_7-CAP, C_{18}-R_7-CAP and C_{20}-R_7-CAP were synthesized according to the procedures described below. The peptides were synthesized following the general procedure described above for peptide 1 using 75 mg of Rink amide resin and three equiv of each amino acid. After the removal of the Fmoc-protecting group from the N-terminal β-alanine, the fatty acid tail was added. Three equiv of the fatty acid were activated with three equiv HCTU and six equiv DIPEA in a 1:1 solution of DCM and DMF and then were added to the resin-bound peptide. The peptides then were cleaved from the resin, isolated, purified as described above, and characterized by MALDI-TOF MS.

Synthesis of C_{14}-βAla-R_7-EDNE-pCAP-TARE-NH_2 and C_{14}-βAla-R_7-EDNE-CAP-TARE-NH_2. C_{14}-βAla-R_7-EDNE-pCAP-TARE-NH_2 (SP1) and C_{14}-βAla-R_7-EDNE-CAP-TARE-NH_2 (CAP-SP1) were purchased from 21st Century Biochemicals or were synthesized following the procedures described above.

Synthesis of C_{14}-βAla-R_7-$(PEG)_4$-REGLN-pCAP-MVLAT-NH_2. C_{14}-βAla-R_7-$(PEG)_4$-REGLN-pCAP-MVLAT-NH_2 (SP2) was purchased from 21st Century Biochemicals.

Quality control of peptides by MS. In the initial batch of SP1, which was used for the experiments in Fig. 2, MS data indicated that the asparagine residue was dehydrated to 3-cyanoalanine. However, we observed no differences in the dephosphorylation of the peptide by CD45 in vitro or in the peptide behavior in cell-based assays compared with the subsequent batches of peptides. In addition, MS data indicated that the SP1 peptide used for the experiments in Fig. 2 was a mixture of the parent peptide and a peptide that was missing one glutamate residue. We did not purify the peptide further because it was used as an internalization control only. All other peptides had unremarkable quality control analysis with purity over 90%.

Purification of Recombinant Proteins. Recombinant LYP, hematopoietic protein tyrosine phosphatase (HePTP), and vaccinia H1-related phosphatase (VHR) were expressed in *Escherichia coli* and purified as described previously (5, 6).

In Vitro Phosphatase Assays. The reactions for in vitro phosphatase assays were performed in triplicate at 37 °C by continuously measuring the change in fluorescence [λ_{exc} = 334 nm and λ_{em} = 460 nm for pCAP substrates and λ_{exc} = 355 nm and λ_{em} = 460 nm for 6,8-difluoro-4-methylumbelliferyl phosphate (DiFMUP) substrates]. For detection of protein tyrosine phosphatase (PTP) activity, enzymes were incubated with substrate in 50 mM Hepes (pH 4.5) with 1 mM DTT and 0.005% (vol/vol) Tween-20. For assays to detect pCAP peptide selectivity, the activity of each PTP was normalized using DiFMUP as a substrate, and equal units were used for the pCAP assays. Assays to determine the IC_{50} of compounds on CD45 were performed using peptide 1 as a substrate. The enzyme was preincubated with increasing concentrations of compound for 40 min. Reactions were initiated by addition of the substrate. To assess the IC_{50} values of the CD45 inhibitors on additional PTPs, DiFMUP was used as a substrate (K_m concentration for each enzyme). Fluorescence was monitored using either a Perkin-Elmer 1420 Multilabel Counter Victor^3 V (Perkin-Elmer) or a Tecan Infinite M1000 (Tecan) plate-reader.

Microinjection of pCAP Peptides to Detect Intracellular PTP Activity. Sea urchin oocytes, which express a wide range of PTPs, including homologs to PTPN22 and SHP-1 (7), were microinjected with peptide 1. Eggs were spawned from an adult sea urchin female. The jelly coat was removed by treatment with acidic seawater (pH 4.0) for 1 min, and eggs were stored at 12 °C until ready for injection. Sperm was collected from adult males and stored at 4 °C until use. Eggs were fertilized in the presence of 150 mM para-aminobenzoic acid seawater and were injected using a Picospritzer (General Valve Corporation) over a Zeiss inverted microscope. To correct for cell/injection volumes, and as an injection marker, fixed amounts of rhodamine were coinjected with the peptides.

Cell Culture and Electroporation. Jurkat cells (8) and the CD45-null Jurkat variant cell line, J45.01 (9), were grown in RPMI medium 1640 with 10% FBS, 1 mM sodium pyruvate, 10 mM Hepes (pH 7.3), 2.5 mg/mL D-glucose, 100 U/mL penicillin, and 100 μg/mL streptomycin. RAW 264.7, COS-7, and J774A.1 cells were grown in DMEM with 10% FBS, 100 U/mL penicillin, and 100 μg/mL streptomycin. For treatment of Jurkat cells with cell-permeable peptides, peptides were added at the appropriate concentration to cells in RPMI with 0.5% FBS, and cells were incubated at 37 °C with 5% CO_2 for the times indicated in the figures. For treatment of COS-7 or RAW 264.7 cells with cell-permeable peptides, cells were plated and allowed to adhere overnight in culture medium. Cells were washed and incubated with appropriate concentrations of peptides in DMEM with 0.5% FBS for the times indicated in the figures. For electroporation experiments, Jurkat cells were washed and resuspended in RPMI without phenol red to a concentration of 50×10^6 cells/mL. A total of 5×10^6 cells per sample was electroporated in the presence of the indicated peptides with an Amaxa Nucleofector Device (Amaxa) using program X-005.

Confocal Microscopy. After treatment with cell-permeable peptides, Jurkat cells were washed and viewed under a Zeiss LSM 510 confocal microscope after spontaneous or cyto-spin–induced adherence to a microscope slide. COS-7 cells were plated in Lab-Tek II chamber slides (Thermo Fisher Scientific) and allowed to adhere overnight in culture medium. CAP fluorescence was detected using a DAPI emission filter.

High-Content Imaging. RAW 264.7 cells were plated in 96-well BD imaging plates (50×10^3 cells per well) and allowed to adhere overnight in culture medium. After incubation with the appropriate concentrations of peptide, cells were washed and fixed for 15 min at room temperature in 3.7% formaldehyde. Cells then were incubated with Sytox Orange and CellMask Deep Red cytoplasmic/nuclear stain (Invitrogen) according to the manufacturer's instructions. Automated image acquisition was performed using the Opera confocal reader [model 3842-Quadruple Excitation High Sensitivity (QEHS); Perkin-Elmer]. Images were acquired from eight fields in a single well and in three independent channels and two exposures. The first exposure used a 640-nm laser to excite CellMask Deep Red cytoplasmic/nuclear stain. The second exposure used a 561-nm laser to excite Sytox Orange and a UV laser for peptide excitation. Images were analyzed within the Opera environment using the standard Acapella scripts. The analysis algorithm was used to identify and segment objects such as nuclei based on Sytox Orange dye and whole cells based on CellMask Deep Red cytoplasmic/nuclear staining. By subtracting the nuclear region from the whole-cell region, a purely cytoplasmic sampling region was generated. The distribution of the fluorescence signal of the dephosphorylated pCAP probe was detected in the signal channel (UV, 425-nm excitation).

Phospho-Flow and T-Cell Activation Assays. Phospho-flow cytometry was performed in Jurkat cells following the manufacturer's protocols (BD Biosciences). The T-cell activation assay was performed by analyzing induction of CD69 expression by FACS following stimulation of Jurkat cells at 37 °C for 4 h with 5 μg/mL plate-bound anti-CD3. Cell fluorescence was assessed on a BD LSR II flow cytometer. The fold induction of CD69 expression was calculated from the ratio of the MFI of each sample to the MFI of the DMSO-treated sample.

Subcellular Fractionation. Jurkat cell lysates were separated into cytosolic and nuclear fractions using the NE-Per Nuclear and Cytoplasmic Extraction Reagents Kit (Thermo Fisher Scientific) according to the manufacturer's instructions.

Anthrax Lethal Toxin Assay. The anthrax lethal toxin assay was performed as described in (3). J774A.1 mouse macrophages were pretreated with medium containing 2% DMSO or the indicated compounds for 1 h. Cells then were treated with anthrax lethal toxin (protective antigen, 80 ng/mL; lethal factor, 16 ng/mL) for 4 h. Then 25 μL of MTT dye (1 mg/mL) was added, and the cells were incubated further for 2 h. The reaction was stopped by adding an equal volume of lysis buffer (50% DMF and 20% SDS, pH 4.7). Plates were incubated overnight at 37 °C, and absorbance was read in a plate-reader at 570 nm.

Graphs and Statistical Analysis. Flow cytometry data analysis and graph preparation were performed using FlowJo software (Tree Star, Inc.). To identify hits in the CD45 inhibitor screen, the percentage of positive cells was calculated for each sample by Overton subtraction (10) between the inhibitor-treated and control cells. The maximum values [average + 3× SD(% of positive cells)] obtained from analyzing at least two multi-replicate experiments on control cells were used as the cutoff. Other graphs, curve fittings, and kinetic parameter calculations were performed using the GraphPad Prism software package (GraphPad). All SDs of differences and ratios were calculated according to the error propagation rules described by Taylor (11).

SI Discussion

As a model system for our assays we used a nine-amino acid peptide derived from the sequence surrounding the activating Tyr394 within the active site of Lck, a T-cell–specific protein tyrosine kinase (PTK). Phosphorylation at this site in T cells is

controlled physiologically by LYP, SHP-1, and CD45 (12). The 9LckpCAP394 (pCAP) peptide was dephosphorylated very efficiently in vitro by recombinant LYP, SHP-1, and CD45 (k_{cat} = 1.5 ± 0.1 s^{-1} and K_m = 3.2 ± 0.4 μM for LYP; k_{cat} = 22.0 ± 0.4 s^{-1} and K_m = 86.9 ± 3.8 μM for SHP-1; k_{cat} = 526.4 ± 22.1 s^{-1} and K_m = 129.3 ± 12.6 μM for CD45).

Two additional sets of preliminary experiments were carried out to show that CAP and pCAP peptides have the necessary selectivity features to be used as probes for intracellular PTP activity. First, CAP peptides were not phosphorylated by PTKs in vitro. To detect whether PTKs were able to phosphorylate coumarin derivatives alone or after their incorporation into peptides, 0.4 mM 4-methylumbelliferone (MU) or various CAP-peptides were incubated with recombinant Csk and Lck in 20 mM Hepes (pH 7.4), 5 mM $MnCl_2$, 20 mM $MgCl_2$, 0.1% Triton-X, 0.1% Nonidet P-40, 1 mM ATP, and 5 mM DTT at 37 °C. The reactions were measured in triplicate by continuously monitoring the fluorescence signal (λ_{exc} = 340 nm and λ_{em} = 460 nm). In addition to MU, we assessed a variety of peptides including KKKKEEI-CAP-FFF [an optimized recognition sequence for Csk (13)] and EEEI-CAP-GVLFKKK [an optimized recognition sequence for Lck (14)]. However, we could not detect any activity of these PTKs on any of these substrates (data not shown). We concluded that the phosphorylation of coumarin derivatives by PTKs is, at best, an unfavorable reaction.

Second, pCAP peptides were not dephosphorylated by serine phosphatases in vitro (Fig. S1). Assays of PP1 activity were conducted in 50 mM Tris·HCl (pH 7.0), 5 mM DTT, 2 mM $MnCl_2$, 0.1 mM EDTA, and 0.2 mg/mL BSA. Assays of PP2A activity were conducted in 50 mM Tris·HCl (pH 7.5), 0.1 mM EDTA, 0.9 mg/mL BSA, 0.09% β-mercaptoethanol, and 1 mM $MnCl_2$. Assays of PP2B activity were conducted in 20 mM Tris·HCl (pH 7.5), 10 mM $MgCl_2$, 0.1 mM $CaCl_2$, 1 mg/mL BSA, and 1 mM DTT. The activity of serine/threonine phosphatases was normalized using DiFMUP as a substrate, and equal units of enzyme were used for the pCAP assays. Fluorescence was monitored using either a Perkin-Elmer 1420 Multilabel Counter Victor^3 V or a Tecan Infinite M1000 plate-reader.

1. Mitra S, Barrios AM (2008) Identifying selective protein tyrosine phosphatase substrates and inhibitors from a fluorogenic, combinatorial peptide library. *ChemBioChem* 9:1216–1219.
2. Panchal RG, et al. (2009) Reduced expression of CD45 protein-tyrosine phosphatase provides protection against anthrax pathogenesis. *J Biol Chem* 284:12874–12885.
3. Panchal RG, et al. (2007) Chemical genetic screening identifies critical pathways in anthrax lethal toxin-induced pathogenesis. *Chem Biol* 14:245–255.
4. Zhang S, et al. (2009) Acquisition of a potent and selective TC-PTP inhibitor via a stepwise fluorophore-tagged combinatorial synthesis and screening strategy. *J Am Chem Soc* 131:13072–13079.
5. Stanford SM, et al. (2011) Discovery of a novel series of inhibitors of lymphoid tyrosine phosphatase with activity in human T cells. *J Med Chem* 54:1640–1654.
6. Wu S, et al. (2009) Multidentate small-molecule inhibitors of vaccinia H1-related (VHR) phosphatase decrease proliferation of cervix cancer cells. *J Med Chem* 52:6716–6723.
7. Byrum CA, et al. (2006) Protein tyrosine and serine-threonine phosphatases in the sea urchin, Strongylocentrotus purpuratus: Identification and potential functions. *Dev Biol* 300:194–218.
8. Abraham RT, Weiss A (2004) Jurkat T cells and development of the T-cell receptor signalling paradigm. *Nat Rev Immunol* 4:301–308.
9. Koretzky GA, Picus J, Schultz T, Weiss A (1991) Tyrosine phosphatase CD45 is required for T-cell antigen receptor and CD2-mediated activation of a protein tyrosine kinase and interleukin 2 production. *Proc Natl Acad Sci USA* 88:2037–2041.
10. Overton WR (1988) Modified histogram subtraction technique for analysis of flow cytometry data. *Cytometry* 9:619–626.
11. Taylor J (1997) *An Introduction to Error Analysis* (University Science Books, Sausalito, CA), 2nd Ed.
12. Zikherman J, et al. (2010) CD45-Csk phosphatase-kinase titration uncouples basal and inducible T cell receptor signaling during thymic development. *Immunity* 32:342–354.
13. Sondhi D, Xu W, Songyang Z, Eck MJ, Cole PA (1998) Peptide and protein phosphorylation by protein tyrosine kinase Csk: Insights into specificity and mechanism. *Biochemistry* 37:165–172.
14. Songyang Z, et al. (1995) Catalytic specificity of protein-tyrosine kinases is critical for selective signalling. *Nature* 373:536–539.

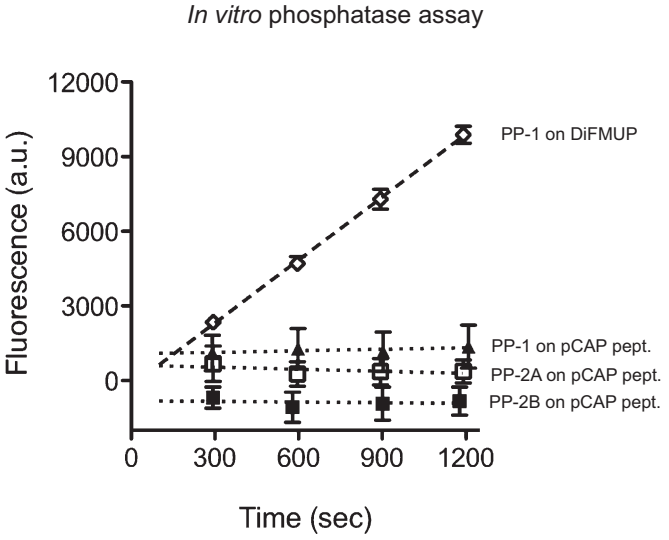

Fig. S1. pCAP peptides are not dephosphorylated by serine/threonine phosphatases. In vitro assay to measure dephosphorylation of 0.2 mM peptide 1 by PP1 (filled triangles), PP2A (open squares), or PP2B (filled squares). Graph shows fluorescence versus time with linear regressions. Open diamonds and dashed line show activity of enzymes on 0.2 mM DiFMUP.

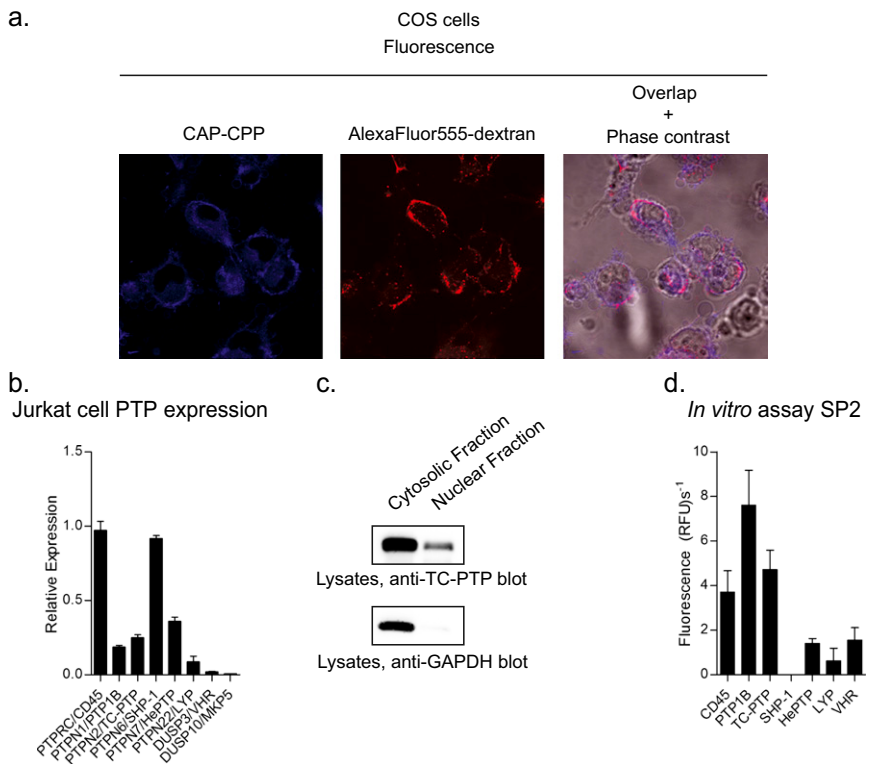

Fig. S2. Intracellular distribution and selectivity of the cell-permeable probes. (*A*) Cytosolic distribution of the probe. COS-7 cells were incubated in medium containing 12.5 μM CAP-containing CAP-CPP and 2.5 mg/mL Alexa Fluor 555-dextran as an endocytosis marker. Images of cells were taken on a confocal microscope after 1 h incubation. Figure shows CAP fluorescence (*Left*), dextran fluorescence (*Center*), and overlap with phase contrast (*Right*). Notice the nuclear exclusion and the cytosolic leakage (regions without colocalization with dextran) of CAP fluorescence. (*B*) Expression of PTPs prominent in Jurkat cells. Graph shows average ± SD of the relative mRNA expression of *PTPRC*/CD45, *PTPN1*/PTP1B, *PTPN2*/TC-PTP, *PTPN6*/SHP-1, *PTPN7*/HePTP, *PTPN22*/LYP, *DUSP3*/VHR, and *DUSP10*/MKP-5 as assessed by quantitative PCR. (*C*) Cytosolic and nuclear localization of TC-PTP. Jurkat cell lysates were separated into cytosolic and nuclear fractions. Panels show Western blotting for TC-PTP and GAPDH. (*D*) The cell-permeable probe SP2 assay is selective for TC-PTP, PTP1B, and CD45. In vitro phosphatase assay to measure dephosphorylation of 0.1 mM SP2 by CD45, PTP1B, TC-PTP, SHP-1, HePTP, LYP and VHR. Graph shows mean ± SD of relative fluorescence units (RFUs)/s.

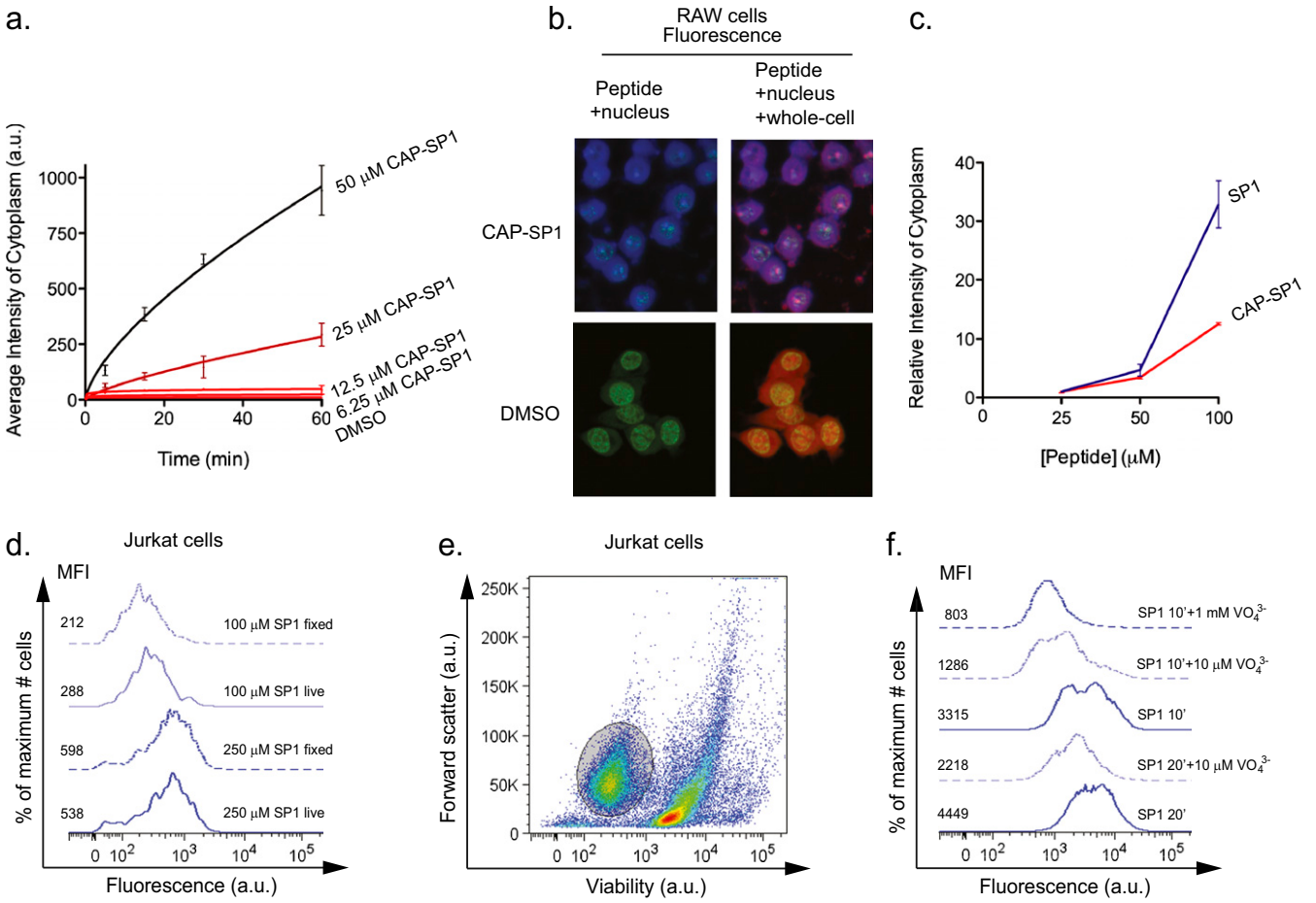

Fig. S3. High-content imaging and flow cytometry detection of internalization and dephosphorylation of cell-permeable fluorogenic PTP activity probes. (*A* and *B*) High-content imaging analysis of dose- and time-dependent internalization of CAP-SP1. (*A*) Average cytoplasmic intensity of RAW 264.7 cells incubated with DMSO alone or increasing concentrations of CAP-SP1 for 5 min, 15 min, 30 min, and 60 min. Nonlinear fitting of the data points is shown, and increasing color intensity indicates increasing concentration of peptide. (*B*) Intracellular peptide fluorescence from fixed cells can be detected by high-content imaging. RAW 264.7 cells were treated with 50 μM CAP-SP1 or DMSO for 1 h. Fluorescence of CAP, nuclei, and whole cells is pseudocolored blue, green, and red, respectively. (*C*) Intracellular dephosphorylation of cell-permeable pCAP peptide depends upon peptide concentration. RAW 264.7 cells were incubated for 1 h with three different concentrations of SP1 (blue line) or CAP-SP1 (red line). Graph shows relative cytoplasmic intensity of cells, using the intensity of cells treated with the lowest amount of peptide as a standard. Notice the different increases in the slope of the connecting lines between the SP1 and CAP-SP1 peptides when the concentration of peptide increases, indicating intracellular dephosphorylation of leaked peptide. (*D–F*) Flow cytometry analysis of pCAP intracellular dephosphorylation. (*D*) Fixation does not interfere with intracellular peptide fluorescence. Jurkat cells were incubated for 30 min with 100 μM (light blue lines) or 250 μM (dark blue lines) SP1. Cells subsequently were washed, fixed in 1% paraformaldehyde (PFA) for 15 min at room temperature (dashed lines) or left without fixation (continuous lines), and were stained with the LIVE/DEAD Fixable Red Dead Cell Stain Kit. Cell fluorescence was analyzed by FACS. Graph shows fluorescence of viable cells. a.u., arbitrary units; MFI, median fluorescence intensity. (*E*) Gating strategy to identify viable cells. After incubation for 30 min with 250 μM SP1, Jurkat cells were washed, fixed in 1% PFA for 15 min at room temperature, and stained with the LIVE/DEAD Fixable Red Dead Cell Stain Kit. Plot shows viability of cells versus forward scatter. Oval shows gating to include viable cells. (*F*) Jurkat cells were preincubated for 30 min with 10 μM vanadate (dashed light blue lines), 1 mM vanadate (dashed dark blue lines), or buffer alone (continuous dark blue lines), followed by incubation with 250 μM pCAP-CPP for 10 or 20 min. Graph shows cell fluorescence as analyzed by FACS.

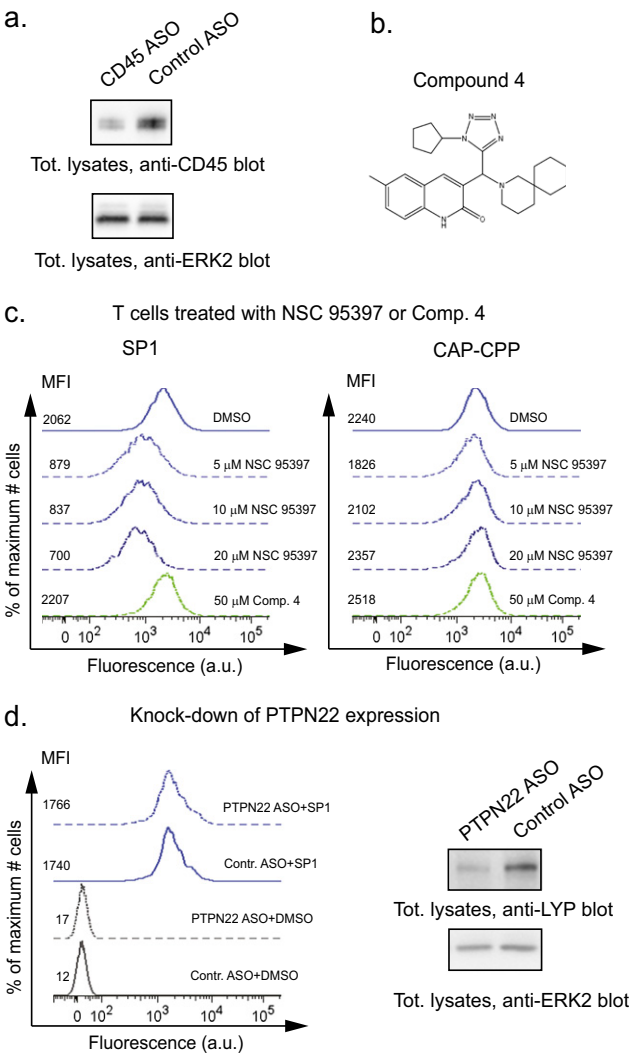

Fig. S4. The CD45 assay does not detect inhibition of LYP. (*A*) Knockdown of CD45 expression by the CD45 antisense oligonucleotide (ASO). Jurkat cells were incubated for 48 h with 10 μM CD45-targeted ASO (CD45 ASO) or control ASO. Western blotting of cell lysates is shown. (*B*) Structure of the LYP-selective inhibitor compound 4. (*C*) Jurkat cells were preincubated for 30 min with 5 μM (dashed light blue lines), 10 μM (dashed blue lines), or 20 μM (dashed dark blue lines) NSC 95397, 50 μM of the LYP-selective inhibitor compound 4 (green lines), or with DMSO (continuous dark blue lines). (*Left*) Fluorescence of cells after incubation with 250 μM SP1 for 10 min. (*Right*) Fluorescence of cells after incubation with 25 μM CAP-CPP for 10 min. (*D*) The CD45 assay does not detect knockdown of LYP expression. Jurkat cells were incubated for 48 h with 10 μM PTPN22-targeted ASO (PTPN22 ASO) or control ASO. (*Left*) Fluorescence of cells after incubation with 250 μM SP1 for 10 min (blue lines) or DMSO alone (gray lines). (*Right*) Western blotting of cell lysates from the same samples.

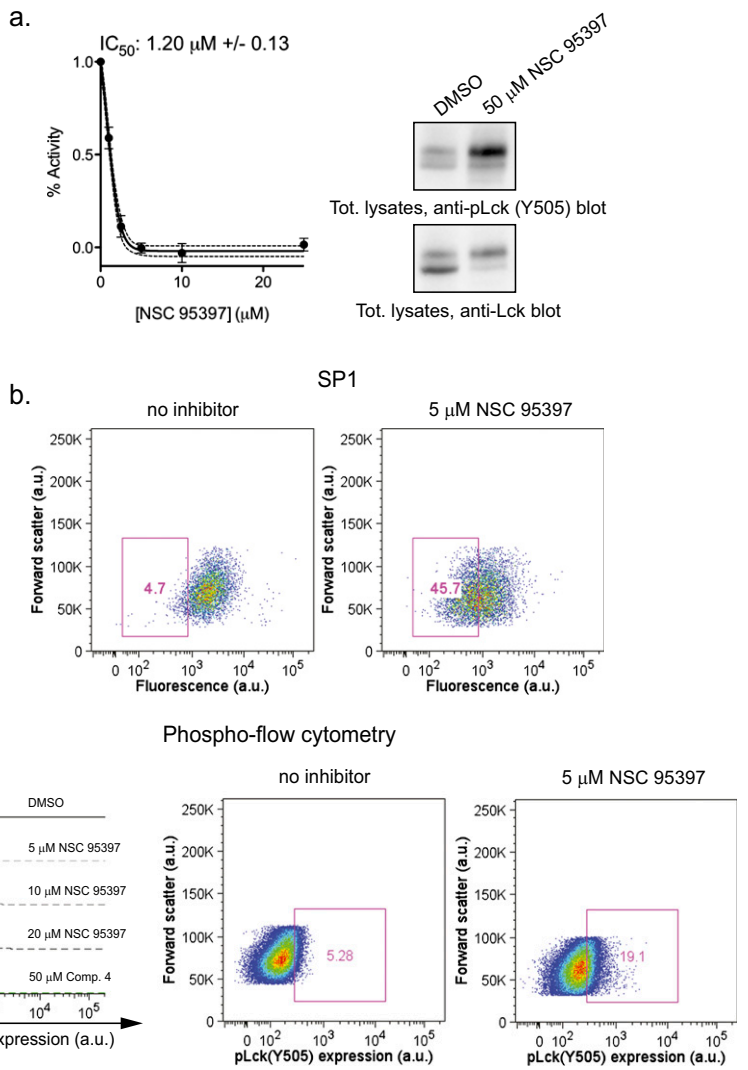

Fig. S5. Signal-to-background ratio of the pCAP cell-based assay is comparable, if not superior, to phospho-flow cytometry and Western blotting analyses. (*A*) (*Left*) In vitro inhibition of CD45 by NSC 95397. Dephosphorylation of 105.9 μM peptide 1 by 2.5 nM CD45 was measured in the presence of increasing concentrations of NSC 95397. Graph shows percent activity versus inhibitor concentration. (*Right*) Detection of CD45 inhibition by Western blotting. Jurkat cells were preincubated for 30 min with 50 μM NSC 95397. (*Upper*) Western blotting of lysates with an anti-pLck (Y505) antibody. (*Lower*) Control anti-Lck blot. (*B*) Detection of CD45 inhibition by the single-cell pCAP assay. Jurkat cells were preincubated for 30 min with DMSO (*Left*) or 5 μM NSC 95397 (*Right*). Plots show fluorescence versus forward scatter of viable cells after incubation with 250 μM SP1 peptide for 10 min. Boxed area (gate) within each panel includes cells with fluorescence equal to or lower than the lower 5% of cells treated with DMSO alone. Percentage of cells within gates is shown. (*C*) Detection of CD45 inhibition by phospho-flow cytometry. (*Left*) Fluorescence of Jurkat cells preincubated for 30 min with 5 μM (dashed light gray line), 10 μM (dashed gray line), or 20 μM (dashed black line) NSC 95397, 50 μM compound 4 (green line), or DMSO (continuous black line) and stained with anti-pLck (Y505) antibody. (*Middle* and *Right*) Jurkat cells were preincubated for 30 min with DMSO (*Left*) or 5 μM NSC 95397 (*Right*). Panels show fluorescence versus forward scatter of viable cells after staining with anti-pLck (Y505) antibody. Boxed area (gate) within each panel includes cells with fluorescence equal to or higher than the upper 5% of cells treated with DMSO alone. Percentage of cells within gates is shown.

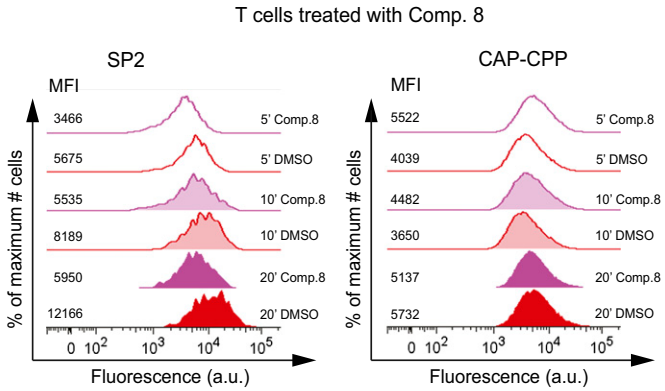

Fig. S6. Single-cell assay to detect intracellular TC-PTP activity. The single-cell assay for TC-PTP activity detects inhibition of TC-PTP by a known cell-permeable compound. Jurkat cells were preincubated for 30 min with 5 nM compound 8 (pink graphs) or with DMSO alone (red graphs). (*Left*) Fluorescence of cells after incubation with 250 μM SP2 for 5 min (open graphs), 10 min (shaded graphs), or 20 min (solid graphs). (*Right*) Fluorescence of cells after incubation with 25 μM CAP-CPP for 5 min (open graphs), 10 min (shaded graphs), or 20 min (solid graphs).

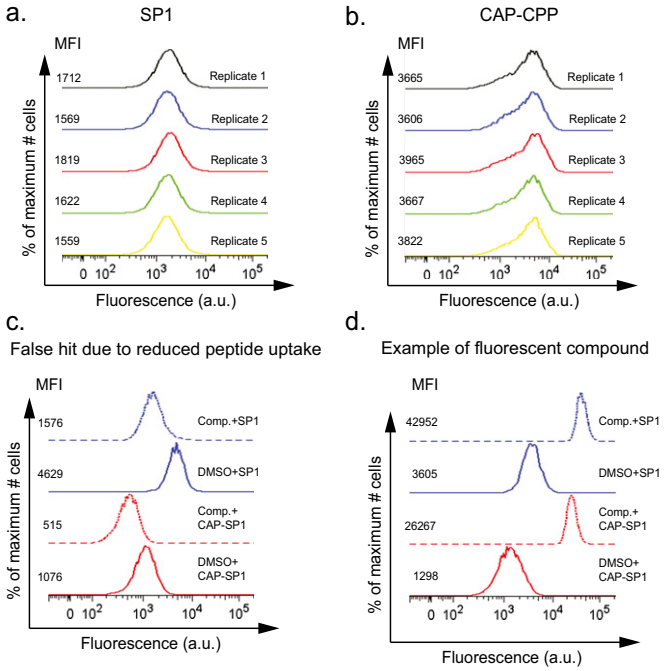

Fig. S7. Small-molecule screening with the pCAP cell-based assay. (*A* and *B*) Stability of the pCAP and CAP peptide assays. Fluorescence of cells after incubation for 10 min with 250 μM SP1 (*A*) or 25 μM CAP-CPP (*B*). Five independent samples are shown. (*C* and *D*) Fluorescent artifacts identified during the screen. (*C*) Example of a representative compound that decreases uptake of the cell-permeable peptide substrate. Graphs show fluorescence of cells preincubated with 10 μM test compound (dashed lines) or DMSO (continuous lines) and incubated for 10 min with 250 μM SP1 peptide (blue lines) or 25 μM CAP-CPP peptide (red lines). (*D*) Example of a representative fluorescent compound. Graphs show fluorescence of cells preincubated with 10 μM test compound (dashed lines) or DMSO (continuous lines) and incubated for 10 min with 250 μM SP1 peptide (blue lines) or 25 μM CAP-CPP peptide (red lines).

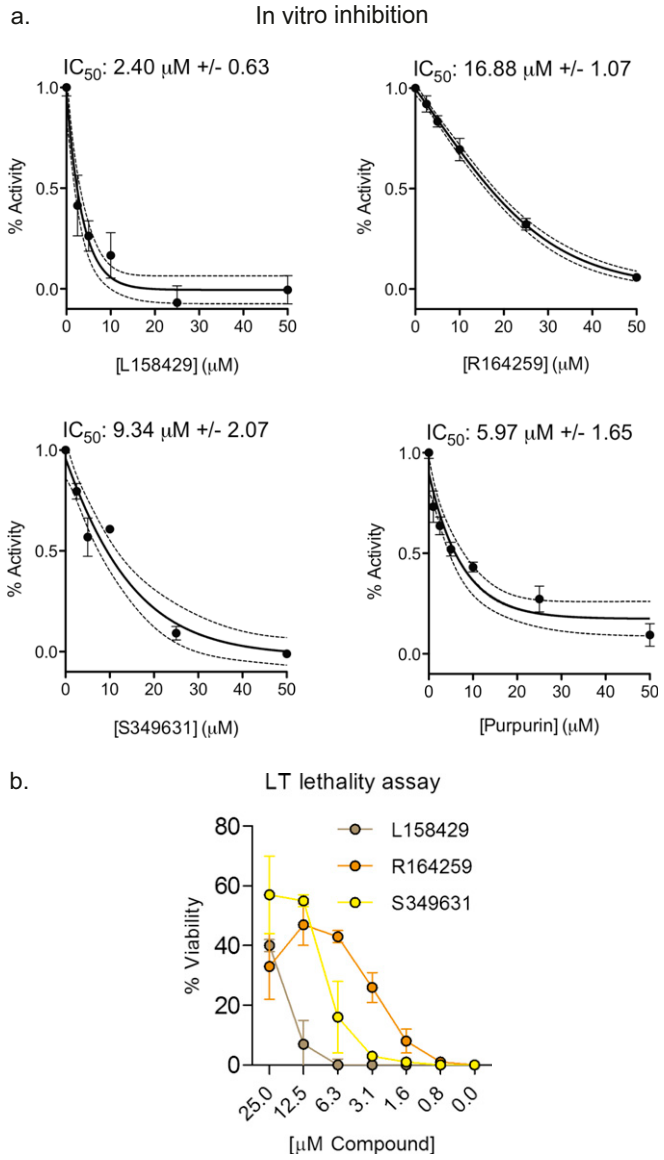

Fig. S8. Validation of small-molecule CD45 inhibitors. (*A*) In vitro inhibition of CD45 by screen hit compounds. Dephosphorylation of peptide 1 by 2.5 nM CD45 was measured in the presence of increasing concentrations of L158429, R164259, S349631, or purpurin. Graphs show percent activity versus inhibitor concentration. (*B*) Small-molecule inhibitors of CD45 protect macrophages from anthrax LT-induced cell death. J774A.1 cells were preincubated with increasing concentrations of the CD45 inhibitors L158429, R164259, or S349631 for 1 h. Cells were then challenged with anthrax LT for 4 h, and cell viability was measured by MTT assay. Graph shows percent viability versus inhibitor concentration.

Table S1. Selectivity of CD45 inhibitors against a panel of PTPs

PTP	L158429 IC_{50} (μM)	R164259 IC_{50} (μM)	S349631 IC_{50} (μM)	Purpurin IC_{50} (μM)
PTP1B	17.4 ± 5.3	10.1 ± 1.9	11.5 ± 1.8	6.0 ± 1.3
HePTP	9.7*	>50	18.2 ± 9.0	8.5 ± 3.2
LYP	> 50	>50	42.8*	10.2 ± 5.2
TC-PTP	19.3 ± 4.7	>50	>50	3.4 ± 1.3
SHP-1	>50	>50	>50	38.9*
VHR	>50	>50	>50	>50

Enzymes were incubated with DiFMUP (K_m concentration for each enzyme) and increasing concentrations of inhibitor in 50 mM Hepes (pH 4.5) with 1 mM DTT and 0.005% Tween-20 at 37 °C. IC_{50} values ± 95% confidence intervals are shown.

*Partial inhibitor; confidence interval could not be calculated precisely.

Table S2. Sequences of the peptides used in this study

Peptide Name	Sequence
peptide 1	Ac-EDNE-pCAP-TARE-NH_2
peptide 1b	Ac-EDNE-CAP-TARE-NH_2
peptide 1c	Ac-EDNE-Et_2pCAP-TARE-NH_2
CAP-R8	Ac-CAP-$(R)_8$
CAP-CPP (C14-R7-CAP)	myristoyl-βAla-$(R)_7$-CAP-NH_2
C16-R7-CAP	C_{16}-βAla-$(R)_7$-CAP-NH_2
C18-R7-CAP	C_{18}-βAla-$(R)_7$-CAP-NH_2
C20-R7-CAP	C_{20}-βAla-$(R)_7$-CAP-NH_2
SP1	myristoyl-βAla $(R)_7$-EDNE-(pCAP)-TARE-NH_2
SP2	myristoyl-βAla-$(R)_7$-$(PEG)_4$-REGLN-(pCAP)-MVLAT-NH_2
CAP-SP1	myristoyl-βAla-$(R)_7$-EDNE-(CAP)-TARE-NH_2